propagation wave number of the exciting field, a and b are the periods of the structure in x and y.

In the case of a structure in free space which is periodic (with period a) in x and arbitrary in y, the free space modes are modified by replacing the normalization factor 2π by $\sqrt{2\pi a}$ and recognizing that the wave numbers k_{xi}' and k_{xi}'' take on the discrete values

$$k_{xi}' = k_{xi}'' = \frac{2m\pi}{a} + k_{x0}, \quad m = 0, \pm 1, \pm 2, \cdots,$$

while the wave numbers k_{yi}' and k_{yi}'' are given by

$$k_{yi}' = k_{yi}'' = \eta + k_{y0}, \quad -\infty < \eta < \infty.$$

These modes are orthogonal in the strip $-a/2 < x < a/2$ and $-\infty < y < \infty$. In the special case of a structure periodic in x but uniform in y, such as an infinite strip grating, the normalization factor is taken as $\sqrt{a}$, and $\eta = 0$. The exponential y dependence is suppressed.

ACKNOWLEDGMENT

The authors wish to express their appreciation to Dr. N. Marcuvitz and A. D. Bresler for helpful discussions and suggestions in connection with this work.

Reflectors for a Microwave Fabry-Perot Interferometer*

W. CULSHAW†

Summary—**The advantages of microwave interferometers for wavelength and other measurements at millimeter wavelengths are indicated, and a microwave Fabry-Perot interferometer discussed in detail. Analogous to the cavity resonator, this requires reflectors of high reflectivity, small absorption, and adequate size. Stacked dielectric plates, and stacked planar or rod gratings are shown to be suitable forms of reflectors, and equations for the reflectivity, optimum spacing, and bandwidth of such structures are derived. A series of stacked metal plates with regularly spaced holes represents a good design of reflector for very small wavelengths. Fringes and wavelength measurements at 8-mm wavelength are given for one design of interferometer, these being accurate to 1 in 10^4 without any diffraction correction. For larger apertures and reflectors in terms of the wavelength, errors due to diffraction will decrease.**

I. INTRODUCTION

IN conjunction with the efforts directed toward the generation and use of shorter wavelengths in the millimeter region, it is necessary to develop new techniques of transmission and measurement. The facility with which methods based on optical techniques can be used for this purpose improves as the wavelength decreases, in contrast to the conventional waveguide methods, where the dimensions of cavity resonators and other components are in general comparable with the wavelength, with a consequent increase in attenuation and fabrication difficulties. Wavelength measurements can be made with interferometers based on optical principles, and at wavelengths around a few millimeters, such methods would be preferable to the use of a cavity resonator.

* Manuscript received by the PGMTT, July 10, 1958; revised manuscript received, November 10, 1958.

† National Bureau of Standards, Boulder Laboratories, Boulder, Colo.

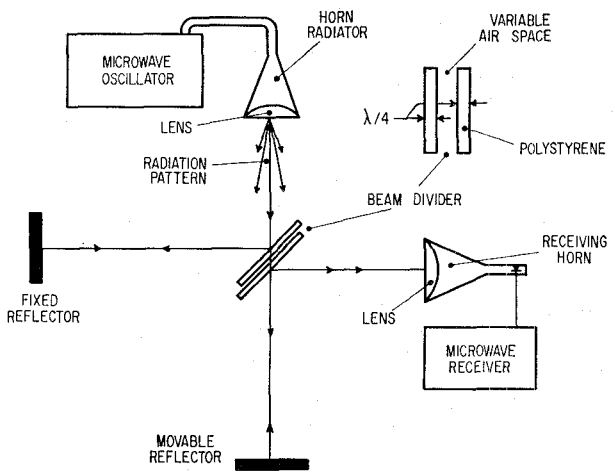

Fig. 1—Microwave form of Michelson interferometer.

A free-space form of Michelson interferometer is shown in Fig. 1; here the beam from the radiating horn is divided by the beam divider into two beams which travel different paths. The two beams then are recombined in the receiving horn, and interference is observed between the two sinusoidal wave trains as one of the reflectors is moved. This interferometer has been operated at $\lambda = 1.25$ cm,[1] the wavelength measurements with a particular form being accurate to a few parts in 10^4 without any correction for diffraction. The free-space beam divider and reference arm can be replaced by a hybrid tee at these wavelengths, and then only a single radiator and reflector are required for the open arm.

[1] W. Culshaw, "The Michelson interferometer at millimeter wavelengths," *Proc. Phys. Soc. B*, vol. 63, pp. 939–954; November, 1950.

Such an interferometer was used by Froome for the accurate determination of the velocity of electromagnetic waves by microwave interferometry.[2] By applying a diffraction correction for the open arm of the interferometer, he obtained a result in agreement with recent determinations by other methods, including the cavity resonator.[3]

Microwave inferferometers can also be used with advantage at wavelengths around 1 cm and below for the measurement of dielectric constants, and at very short wavelengths would again be preferable. Both the Michelson and Fabry-Perot types of interferometer have been used for this purpose,[1,4] and more recently Blair[5] has described a microwave interferometer designed specifically for the measurement of dielectric constants of materials in sheet form at wavelengths around 3 cm.

The fringes in the Michelson interferometer are due to the interference of two wave trains, and for maximum sensitivity the beams must be accurately balanced to give a sharp null. In the Fabry-Perot interferometer shown in Fig. 2 the fringes are made very sharp by multiple reflections between two highly reflecting surfaces, and in the microwave region it represents the free-space analog of the cavity resonator. The narrow bright rings in the optical form of this interferometer show the increased resolution possible.[6] The principle of the microwave form is exactly analogous, though the technique of reflector design is different because any metallic film would seriously attenuate the microwave radiation. Also, we deal essentially with a single plane-wave train in the microwave form so that the circular fringe system is not obtained, except that the distance d between the reflectors can be adjusted to pass various portions of the continuous plane-wave spectrum radiated by the aperture.

To obtain high sensitivity in this interferometer the reflectivity of the reflectors must approximate that of metals such as silver, and undue attenuation in the reflector system must be avoided. The reflectors and apertures used must also be large compared with the wavelength, so that errors in the wavelength measurement due to diffraction are reduced, and their consideration facilitated as required in work of high precision. We shall be mainly concerned with ways of meeting these requirements on the reflectors, bearing in mind that any reflector technique developed should be applicable to wavelengths extending down to 1 millimeter and below, when adequate sources are available.

[2] K. D. Froome, "Determination of the velocity of short electromagnetic waves by interferometry," *Proc. Roy. Soc. A*, vol. 213, pp. 123–141; 1952.

[3] L. Essen, "The velocity of propagation of electromagnetic waves derived from the resonant frequencies of a cylindrical cavity resonator," *Proc. Roy. Soc. A*, vol. 204, pp. 260–277; December, 1950.

[4] W. Culshaw, "The Fabry-Perot interferometer at millimeter wavelengths," *Proc. Phys. Soc. B*, vol. 66, pp. 597–608; July, 1953.

[5] G. R. Blair, "An ultra-precise microwave interferometer," 1958 IRE National Convention Record, pt. 1, pp. 48–56.

[6] F. A. Jenkins and H. E. White, "Fundamentals of Optics," McGraw-Hill Book Co., Inc., New York, N. Y., pp. 269–274; 1950.

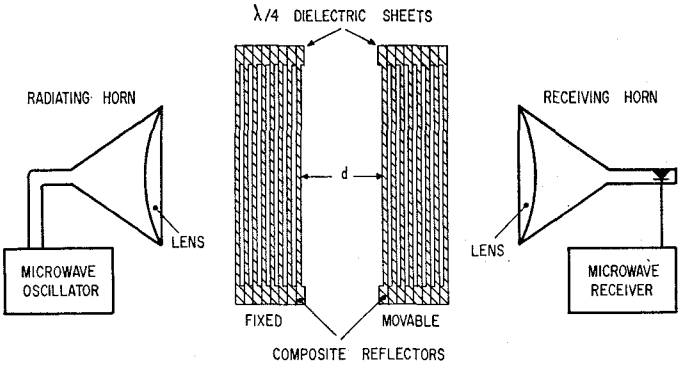

Fig. 2—Microwave Fabry-Perot interferometer.

The theory of the Fabry-Perot interferometer as applied to the microwave region will be dealt with first, together with the theory necessary for the consideration of composite reflecting systems. These will consist of lattice structures such as stacked dielectric plates, stacked metal rod gratings, and stacked metal plates with holes in them.

II. The Fabry-Perot Interferometer

An arrangement of this is shown in Fig. 2, electromagnetic horn radiators with lenses being used to produce efficient radiating and receiving apertures. Radiated energy passes between the reflectors, represented by the dielectric sheet reflectors shown, and at certain spacings of the reflectors, separated by $\lambda/2$ intervals, the multiply reflected waves reinforce each other to give a sharp transmitted fringe. The sharpness of the fringe as d varies depends on the reflectivity obtained, and on the angular width of the radiated and received spectra, since d can be optimized for each plane wave in the spectrum. This interferometer is basically quite simple, it does not require any form of beam divider, and the problem of preserving a balance with displacement between two interfering beams, as in the Michelson type, does not arise. It is, however, necessary to use highly reflecting devices for the reflectors, as the setting accuracy and the diffraction correction will depend on this.

The theory of operation of the interferometer may be developed using transmission line theory. Referring to Fig. 3, the general transmission line matrix of the symmetrical four terminal network may be written

$$\begin{bmatrix} V_{n+1} \\ I_{n+1} \end{bmatrix} = \begin{bmatrix} A & B \\ C & A \end{bmatrix} \begin{bmatrix} V_n \\ I_n \end{bmatrix}. \tag{1}$$

For matched conditions at the output, and all impedances normalized with respect to the characteristic impedance of the line, the input impedance Z_{in} may be determined. The voltage amplitude reflection coefficient is then,

$$r_v = \frac{B - C}{2A + B + C}, \tag{2}$$

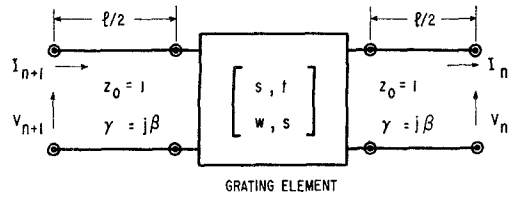

Fig. 3—Line symmetrically loaded by transmission matrix of grating element.

and the ratio of the voltage or current at the output terminals to the incident voltage or current is given by

$$t = \frac{2}{2A + B + C}. \tag{3}$$

Assuming a single plane wave propagating along its axis, the equation governing the transmission and reflection in the complete interferometer may be written in matrix form as

$$\begin{bmatrix} V_{n+1} \\ I_{n+1} \end{bmatrix} = \begin{bmatrix} a & b \\ c & a \end{bmatrix} \begin{bmatrix} \cosh \gamma d & \sinh \gamma d \\ \sinh \gamma d & \cosh \gamma d \end{bmatrix} \begin{bmatrix} a & b \\ c & a \end{bmatrix} \begin{bmatrix} V_n \\ I_n \end{bmatrix}, \tag{4}$$

where the elements a, b, and c, refer to the symmetrical reflectors, $\gamma = \alpha + j\beta$ is the propagation constant for the medium between the reflectors, and d is the distance between them. With matched conditions at the output terminals, the condition for no reflection from the interferometer is

$$\tanh \gamma d = -\frac{2a}{b + c}. \tag{5}$$

At this separation the whole system is matched, and assuming no loss in the reflectors or in the medium between them, the modulus of the transmission coefficient is unity.

Using (4), and substituting the matrix elements corresponding to A, B, and C in (2) and (3), the reflection and transmission coefficients of the interferometer, r_I and t_I, may be determined. For no loss in the reflectors, and with $\gamma = j\beta$ these may be written

$$|r_I|^2 = \frac{4R \sin^2 \phi}{1 - 2R \cos 2\phi + R^2} \tag{6}$$

$$|t_I|^2 = \frac{(1 - R)^2}{1 - 2R \cos 2\phi + R^2} \tag{7}$$

where

$$\phi = (\beta d + \psi), \qquad R = |r|^2,$$

and

$$|r| \exp(-j\psi) = j(b - c)/[2a + j(b + c)].$$

Hence $|t_I|^2$ and $|r_I|^2$ have maximum values when

$$\phi = n\pi, \quad \text{and} \quad \phi = (2n + 1)\pi/2 \tag{8}$$

respectively, where n is the order of interference.

Eqs. (6) and (7) show that the sharpness of the fringes depends on the value of reflection coefficient, R, obtained, and some fringe shapes for various reflectivities are shown in Fig. 4. For precise work high reflectivity must be used since the discrimination with d, or setting accuracy achieved, will depend on this. A measure of the fringe sharpness may be obtained by deducing the Q factor of the reflectors from (7), since the value of ϕ at which the transmitted power is half the maximum is given by

$$\cos 2\phi_1 = [2R - (1 - R)^2]/2R. \tag{9}$$

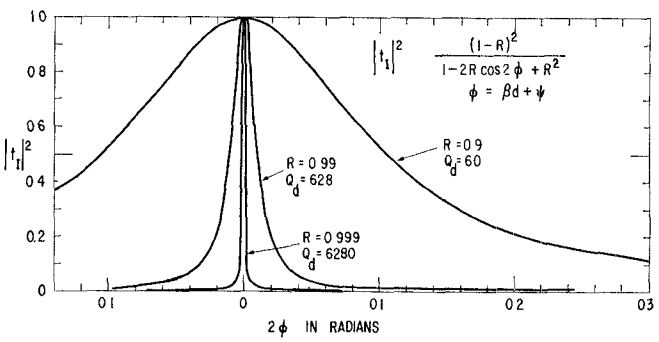

Fig. 4—Variation of fringe sharpness with reflectivity.

The change in βd required to obtain the angle ϕ_1, can be effected by changing the wavelength, or the spacing of the reflectors, and the respective Q values deduced are

$$Q_\lambda = \frac{\lambda}{2\Delta\lambda} = \frac{1}{2\phi_1}(n\pi - \psi)$$

and

$$Q_d = \frac{\lambda}{2\Delta d} = \frac{\pi}{\phi_1}. \tag{10}$$

Actually instead of the single plane wave assumed so far, the aperture will radiate an angular spectrum of plane waves determined by its size, and its field distribution. The portion of this angular spectrum which is effective between the reflectors at any particular spacing d may be deduced from (8) and (10), since a wave traveling at an angle θ to the axis corresponds to a change in path length given by

$$\Delta d = d(1 - \cos \theta), \tag{11}$$

and can also be regarded as a change in effective wavelength to $\lambda/\cos\theta$. As an approximation considering only those waves propagated between the positions of half-maximum intensity the result is

$$\cos \theta = 1 - 1/2Q_\lambda, \tag{12}$$

which shows that the higher the reflectivity, the smaller the number of plane waves which are transmitted through the interferometer at optimum, and other spacings of the reflectors.

For reflectors very large compared with the wavelength, the angular width of the plane-wave spectra generated will correspond to the radiation pattern of the horns, and depending on the reflectivity as indicated by (12), a number of these will be passed by the reflector system at any particular distance d, the reflector system thus acting as a plane-wave filter. The summation of the plane waves which pass through the complete interferometer will lead to an optimum setting slightly different from that given by (8), which assumes a single plane wave along the axis, and in the measurement of length with the interferometer the diffraction correction is the difference between the errors due to the two summations of plane waves effective in the interferometer at the initial and final reflector separations used. The correction can be made small if the reflectivity and order of interference used are such that θ becomes a very small angle. In general, for the high values of reflectivity discussed later, and apertures and reflectors some 15 wavelengths in extent, it is found experimentally that the error due to diffraction in a wavelength measurement on the interferometer is around a part in 10^4. For apertures and reflectors larger in terms of wavelengths the error would decrease. Some quantitative discussion on the diffraction correction could be made using (7) to find the transmission coefficient through the interferometer for different distances d and reflectivities. The radiated and received angular spectra of the apertures, their distances from the reflectors, and the reflector size would also have to be considered.

III. Theory of Reflector Design

One type of reflector which has been used[4] is shown in Fig. 2, and consists of a number of quarter-wave plates of dielectric with quarter-wave air spacings between them. If ϵ is the dielectric constant and zero dielectric loss is assumed, the amplitude reflection coefficient from n such sheets and spacings is equal to that of a single quarter-wave sheet having a dielectric constant of ϵ^n. In view of the high reflectivities involved, however, the effect of a finite dielectric loss must be considered, and it is found[4] that if A_1 refers to the amplitude reflection coefficient from a single quarter-wave sheet, and A_n that from n such sheets with quarter-wavelength spacings between them, then

$$A_{n+1} = \frac{A_1 + A_n(R_0^2 + \psi)/(1 + R_0^2\psi)}{1 + A_1 A_n}, \qquad (13)$$

where $A_1 = R_0(1+\psi)/(1+R_0^2\psi)$, $\psi = \exp(-\pi \tan \delta/2)$, $\tan \delta$ is the loss tangent of the dielectric, and R_0 is the amplitude reflection coefficient at the air-dielectric boundary. The effect of dielectric loss is to limit the reflectivity obtainable by stacking such sheets. For polystyrene $\epsilon = 2.56$ and $\tan \delta = 0.001$ approximately, and the values of A_n shown in Table I are obtained, the limiting value being 0.9982.

TABLE I

Values of the Amplitude Reflection Coefficient Obtained from n Quarter-Wave Plates of Polystyrene with $\lambda/4$ Air Space Between Them.

n	1	2	3	4	5	6	7	8
A_n	0.4378	0.7340	0.8861	0.9528	0.9806	0.9913	0.9961	0.9977

Fig. 5 shows the fringes obtained, at given spacings of the reflectors, as d is varied for an interferometer with reflectors consisting of eight such plates of polystyrene.[4] These had a diameter of about 11 inches, the radiating and receiving apertures being 6 inches square, and the wavelength around 8.33 mm. The sharpness of the fringes illustrates the potentialities of this interferometer for accurate measurements at very short wavelengths. For a dielectric with smaller loss and higher dielectric constant, such as fused quartz, higher values of reflectivity can be obtained. Such reflectors would be very costly due to the required size, except at very short wavelengths, but here the reflector plates become very thin. Odd multiples of quarter wavelength may be used, but the ultimate reflectivity obtained and the bandwidth of the reflectors will decrease.

This leads to the consideration of other types of reflectors, such as a stacked system of gratings, consisting of plane layers of inductive, or capacitive, irises or rods placed symmetrically behind each other, similar to the structures used in delay dielectrics.[7] Fig. 3 shows the basic element which can be used for all the structures considered, the particular grating being represented by a discontinuity transmission matrix symmetrically located on a length of parallel plate transmission line. The transmission line matrix representing the discontinuity may be derived from the equivalent networks of the various gratings, and the reflectivity from a finite number of such elements must be determined. Only TEM mode interaction between the gratings is considered, and all other modes on the structure must be evanescent. Since only even order modes are excited on such a symmetrical structure, a spacing between grating elements less than λ is sufficient for this, but in practice a spacing less than $\lambda/2$ is preferable.

The matrix representing the basic element shown in Fig. 3 may be written for a lossless transmission line as,

$$\begin{bmatrix} V_{n+1} \\ I_{n+1} \end{bmatrix} = \begin{bmatrix} s\cos\theta + j/2\sin\theta(t+w), & \cos\theta(w+t)/2 + js\sin\theta - (w-t)/2 \\ \cos\theta(w+t)/2 + js\sin\theta + (w-t)/2, & s\cos\theta + j/2\sin\theta(t+w) \end{bmatrix} \begin{bmatrix} V_n \\ I_n \end{bmatrix} \qquad (14)$$

[7] J. Brown, "Microwave Lenses," Methuen and Co. Ltd., London, Eng., pp. 53–68; 1953.

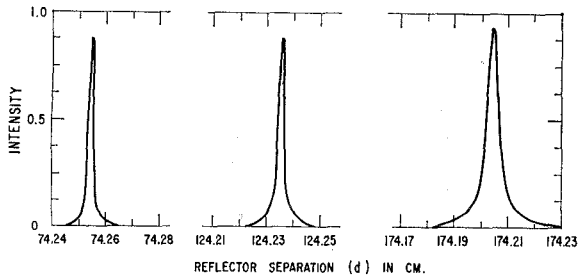

Fig. 5—Fringe shapes measured on microwave Fabry-Perot interferometer.

where $\theta = 2\pi l/\lambda$. Also referring to (2) and (3), and Fig. 6, we obtain for the general four terminal network,

$$\begin{bmatrix} b_{n+1} \\ a_{n+1} \end{bmatrix} = \begin{bmatrix} \frac{B-C}{2}, & \frac{2A-(B+C)}{2} \\ \frac{2A+B+C}{2}, & -\frac{B-C}{2} \end{bmatrix} \begin{bmatrix} b_n \\ a_n \end{bmatrix}, \quad (15)$$

and since $r_{n+1} = b_{n+1}/a_{n+1}$, and $r_n = a_n/b_n$, the recurrence relation between the reflection coefficients for elements in cascade is,

$$r_{n+1} = \frac{[2A-(B+C)]r_n + B - C}{2A + B + C - (B-C)r_n}, \quad (16)$$

and by inserting elements corresponding to A, B, and C, from (14), the reflectivity from a number of basic elements may be determined. The transmission coefficient $t_n = b_n/a_{n+1}$ may also be deduced from (15).

The spacing l between gratings for optimum reflection may be deduced from the equivalent matrix of the basic element by deducing its effective propagation constant Γ, and characteristic impedance Z. Using (1), these are given by[8]

$$\cosh \Gamma l = A, \quad \text{and} \quad Z^2 = B/C \quad (17)$$

and may be determined from (14) for any particular structure. Putting $\phi = \Gamma l$, the over-all matrix for n such structures in cascade may then be written as

$$\begin{bmatrix} V_n \\ I_n \end{bmatrix} = \begin{bmatrix} \cosh n\phi, & Z \sinh n\phi \\ \frac{1}{Z}\sinh n\phi, & \cosh n\phi \end{bmatrix} \begin{bmatrix} V_0 \\ I_0 \end{bmatrix} \quad (18)$$

Consider such a periodic structure, then by (14)

$$\cosh \phi = A = s \cos \theta + j/2 \sin \theta(t + w), \quad (19)$$

and putting $\phi = (\alpha + j\beta)l$, since $\cosh \phi$ must be real, the stop bands of the structure are given by $\sin \beta = 0$, and the pass bands by $\sinh \alpha = 0$. Thus for the pass bands:

$$\cos \beta = A \quad \text{where} \quad |A| < 1, \quad (20)$$

and in the stop bands:

$$\cosh \alpha = |A| \quad \text{where} \quad |A| > 1. \quad (21)$$

[8] L. Brillouin, "Wave Propagation in Periodic Structures," Dover Publications Inc., New York, N. Y., pp. 193–226; 1953.

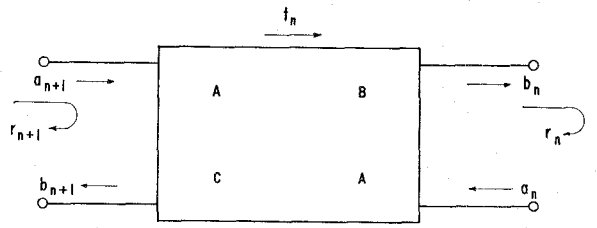

Fig. 6—Reflection and transmission coefficients of four-terminal network.

Thus from (2) and (18), if the spacing l between gratings is such that θ lies within a pass band of the structure, the reflection coefficient r_n becomes

$$r_n = \frac{j(Z^2-1)\sin n\beta}{2Z\cos n\beta + j(Z^2+1)\sin n\beta} \quad (22)$$

while for spacings corresponding to a stop band,

$$r_n = \frac{(Z^2-1)\sinh n\alpha}{2Z\cosh n\alpha + (Z^2+1)\sinh n\alpha}. \quad (23)$$

For spacings such that θ lies within the pass band, the reflection coefficient r_n will oscillate with increase in n, and become zero when $\sin n\beta = 0$. As an example, a thin grating may be represented by an admittance $Y = jB$ on the line and (14) and (20) give

$$\cos \beta = \cos \theta - B/2 \sin \theta \quad (24)$$

and $r_3 = 0$ when $\tan^2 \theta(1-B^2) + 4B \tan \theta - 3 = 0$, with similar results for other values of n.

When l is such that θ lies in the stop band of the structure, the reflectivity will increase monotonically with n, and it is found from (17), (22), and (23) that the spacing for maximum reflectivity, corresponds to the value of θ which gives the maximum value of $\cosh \alpha = |A|$ within the stop band. Eq. (24) is plotted in Fig. 7 for various values of B; for inductive admittances the pass band extends from values of $\theta < \pi$ to $\theta = \pi$, the interval diminishing with increasing values of B. Similar remarks apply to capacitive admittances, the pass band now extending from $\theta = \pi$ to $\theta > \pi$. Thus $l = \lambda/2$ is not a good spacing for gratings of this type since it corresponds to the edge of the pass band and will be frequency sensitive. The spacing for optimum reflection corresponds to the maxima of these curves, which shows that, except for small values of B, a spacing of $l = \lambda/4$ will be satisfactory for thin gratings. For $B = -2$ the pass band extends from $\theta = \pi/2$ to $\theta = \pi$, and Fig. 8 shows the variation in reflectivity, and the zeros which occur within the pass band for different values of n and spacing l. Similar considerations apply to thick gratings, and will be used to optimize the design of reflectors of this type.

IV. Application to Grating Reflectors

A) *Thin Planar Gratings*

Fig. 9 shows a good structure for the reflectors, which consists of a series of circular holes regularly spaced in a

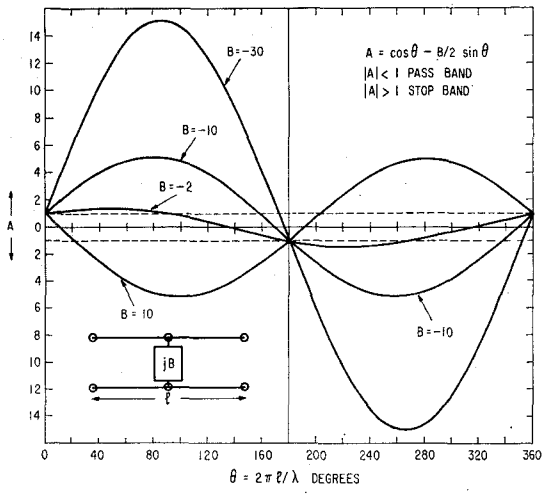

Fig. 7—Pass and stop bands for periodic structure shown.

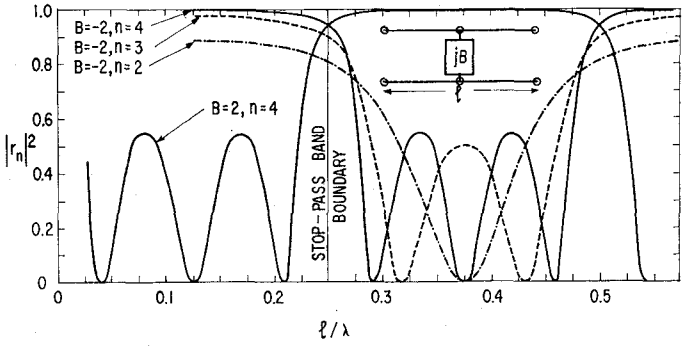

Fig. 8—Reflectivity $|r_n|^2$ versus spacing l for thin gratings, showing oscillations of reflectivity in pass band of structure.

thin metal sheet. Such a system of gratings is equivalent to a number of inductive susceptances across the parallel plate transmission line, and values of the normalized susceptances are given by (25),[9] when the transverse spacings a and b are $<\lambda$, and where R/a and $R/b<1$, R being the hole radius.

$$B = \frac{3ab\lambda}{8\pi R^3} - \frac{72}{\pi\lambda R^2} \cdot \left[\sum_{m=0}^{\infty}{}' \sum_{n=0}^{\infty}{}' (\epsilon_m n^2/b^2 + \epsilon_n m^2/a^2) J^2{}_1(X) \right] \quad (25)$$

where $X = [\pi R(m^2/a^2 + n^2/b^2)]^{1/2}/(m^2/a^2 + n^2/b^2)^{5/2}$, the primes denote summation over even integers only, J_1 is the Bessel function of order unity, and $\epsilon_{m,n} = 1$ if if m, $n = 0$, and $= 2$ if m, $n \neq 0$. For $a/R > 5$ the term $3ab\lambda/8\pi R^3$, which agrees with the usual value of susceptance for such a small hole,[10] is adequate.

Values of the reflectivity $|r_n|^2$ for such a structure, calculated from (16) or (23), are shown in Table II for

[9] J. Munushian, "Electromagnetic Propagation Characteristics of Space Arrays of Apertures-in-Metal Discontinuities and Complementary Structures," University of California, Berkeley, Electronics Res. Lab. Rep., Ser. No. 60, Issue 126; September, 1954.

[10] C. G. Montgomery, R. H. Dicke, and E. M. Purcell, "Principles of Microwave Circuits," M.I.T. Rad. Lab. Ser., McGraw-Hill Book Co., Inc., New York, N. Y., pp. 176–179; 1948.

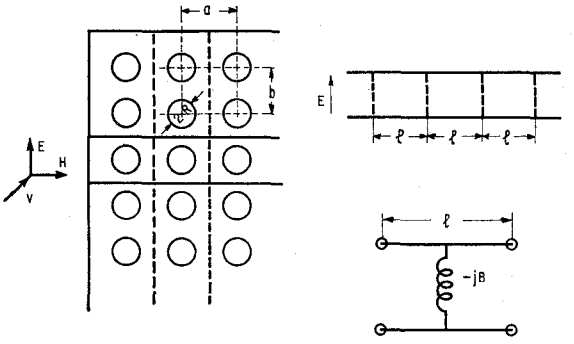

Fig. 9—Thin perforated metal plate gratings and equivalent transmission line circuit. Electric wall ————, magnetic wall – – – – – –.

TABLE II

VALUES OF REFLECTIVITY, $|r_n|^2$, OBTAINED FROM A NUMBER OF THIN INDUCTIVE GRATINGS AT $l = \lambda/4$ SPACING.

n	$B=-2$	$B=-5$	$B=-10$	$B=-30$
1	0.5000	0.86207	0.96154	0.99558
2	0.8000	0.99364	0.99960	0.99999

a spacing l of $\lambda/4$, the reflectivity increasing when further gratings are added. At a wavelength of 6.28 mm, with spacing $a = b = 0.125$ inch, and a hole diameter of 1/16 inch, the normalized susceptance would be around -15, and the attenuation constant for the first higher mode on the structure would be 86 db per wavelength, representing a suitable design for this wavelength.

Similarly the reflectivities possible by stacking inductive or capacitive strip gratings may be calculated using the appropriate formula for the equivalent reactances.[11]

B) Thick Gratings

A capacitive rod type of grating structure is shown in Fig. 10, with the equivalent circuit, the electric vector being perpendicular to the metal rods. Values of the appropriate reactances are given by[12]

$$X_a = -\frac{1}{2}\frac{a}{\pi\beta r^2}\left[1 + \frac{7\beta^2 r^2}{8} + \frac{1}{2}\beta^2 r^2 \ln\left(\frac{2\pi r}{a}\right) - \frac{\pi^2 r^2}{3a^2}\right]$$

$$X_b = -\frac{1}{2}\frac{\pi\beta^2 r^2}{a}\left[1 + \frac{1}{2}\beta^2 r^2 \ln(2\pi r/a) - \frac{3\beta^2 r^2}{8}\right], \quad (26)$$

where $\beta = 2\pi/\lambda$, a is the rod spacing in the grating, and r is the rod radius. Using these values the discontinuity matrix is determined, and substitution of its elements into (17), gives the effective propagation constant, and characteristic impedance of the basic element. The reflectivity follows from (16) or (23), once the spacing for

[11] N. Marcuvitz, "Waveguide Handbook," M.I.T. Rad. Lab. Ser., McGraw-Hill Book Co., New York, N. Y., pp. 280–285; 1951.

[12] L. Lewin, "Advanced Theory of Waveguides," Iliffe and Sons Ltd., London, Eng., pp. 37–44; 1951.

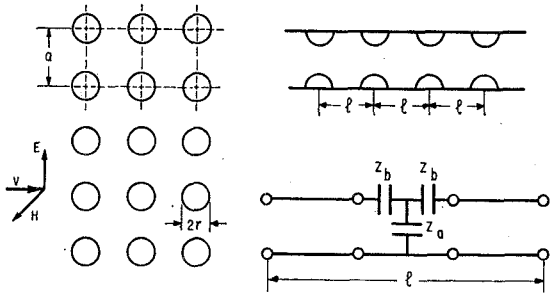

Fig. 10—Stacked capacitive rod gratings and equivalent circuits.

optimum is determined; this is done by finding the value of l which gives the maximum value of cosh α, as indicated in Section III.

Consider a wavelength of 6.28 mm and rods of diameter 0.063 inch, which are readily available, then $r/\lambda = 0.1275$, and for $a/\lambda = 0.417$, (26) gives $X_a = -0.95$ and $X_b = -0.372$, and hence $s = 1.3916$, $t = -0.890j$, and $w = 1.053j$. The effective propagation constant of the basic element is then

$$\cosh \phi = A = 1.3916 \cos \theta - 0.0815 \sin \theta. \quad (27)$$

Fig. 11 shows the variation of A with θ, the optimum value of l being close to $\lambda/2$ for this grating. Values of reflectivity $|r_n|^2$ are shown in Table III for this spacing. A spacing l of $3\lambda/4$ was also considered, but as indicated by Fig. 11, such a spacing is within the pass band of the infinite structure, and is not suitable. The values $|r_1|^2 = 0.48542$ and $|r_2|^2 = 0.0244$ obtained, showed this conclusion to be correct.

At a wavelength of 6 mm the bulk reflectivity $|r|^2$ of silver is around 0.99958, and thus the reflectivity obtained by stacking 5 or 6 such capacitive gratings should be comparable. Losses in the grating elements have been neglected, and will limit the ultimate reflectivity from the structure. For good conductors losses should be small and the values of reflectivity obtained should approach those calculated above. The spacing $a/\lambda = 0.417$ gives an attenuation constant of 100 db per wavelength for the lowest even order TM_{on} mode, and such a structure should adequately satisfy our requirements.

Similarly inductive rod grating structures can be considered using the appropriate equivalent circuits to find the discontinuity matrix.[13] For a spacing of $a/\lambda = 0.417$, and rod diameter given by $d/a = 0.2$, $s = 0.3195$, $t = -0.216j$, and $w = -4.149j$, and the effective propagation constant of the basic element is

$$\cosh \phi = A = 0.3195 \cos \theta + 2.1829 \sin \theta. \quad (28)$$

The curve of this in Fig. 11 shows that $l = \lambda/4$ or $3\lambda/4$ is the optimum spacing for this type, and the values of reflectivity obtained are given in Table IV.

The effect of a finite sheet thickness on the perforated hole grating system can be seen by discussing the similar problem of stacked waveguide hole or iris gratings

[13] Marcuvitz, *op. cit.*, pp. 285–289.

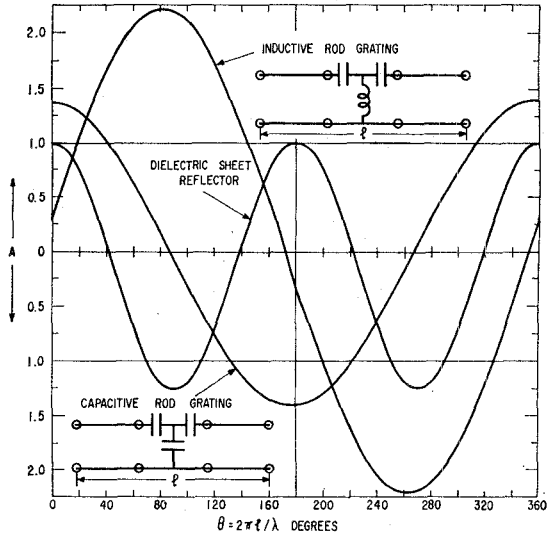

Fig. 11—Pass and stop bands for thick gratings.

TABLE III

CALCULATED REFLECTIVITY $|r_n|^2$ FROM A NUMBER n OF STACKED CAPACITIVE ROD GRATINGS AT $\lambda/2$ SPACINGS. ROD DIAMETER 0.063 INCH, SPACING $a = 0.103$ INCH, $\lambda = 6.28$ MM.

n	1	2	3	4	5	6
$\|r_n\|^2$	0.48542	0.87963	0.97699	0.99583	0.99925	0.99986

TABLE IV

REFLECTIVITY $|r_n|^2$ OF STACKED INDUCTIVE ROD GRATINGS AT $3\lambda/4$ SPACING. ROD DIAMETER $= 0.2\lambda$, SPACING $a = 0.417\lambda$.

n	1	2	3	4
$\|r_n\|^2$	0.794^{88}	0.98660	0.99_8^{76}	0.99992

shown in Fig. 12. Values of the susceptances B_a and B_b of the equivalent circuit, and other parameters are available,[14] and as before it is found that the optimum spacing for this is $l = \lambda_g/4$ or $3\lambda_g/4$, the pass bands being very narrow in the region of $\theta = \pi$ for the parameters $\lambda/a = 1.40$, $a/b = 2$, $d/a = 0.3$, and $t/d = 0.27$, corresponding to an iris thickness of 0.020 inch at $\lambda = 6.28$ mm. Values of reflectivity obtained are higher than those for thin irises of the same hole diameter, which agrees with the usual values of coupling factors for thick irises.[15] The behavior of the thick perforated metal plate gratings will be similar, and the reflectivity from a few of these at $\lambda/4$ or $3\lambda/4$ spacings will be quite high.

An indication of the bandwidth of the various structures is given by the effective propagation constant curves shown in Fig. 7 and Fig. 11; Fig. 13 shows the reflectivity of capacitive and inductive rod gratings as a function of l, and shows that provided a sufficient number of gratings is used the reflectivity obtained will be

[14] Marcuvitz, *op. cit.*, pp. 408–412.
[15] Montgomery *et al.*, *op. cit.*, p. 201.

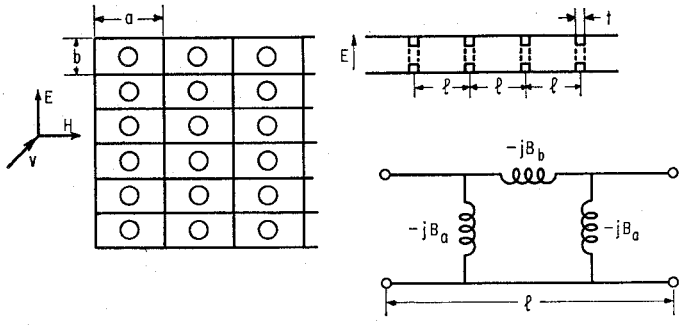

Fig. 12—Waveguide iris gratings and equivalent circuits.

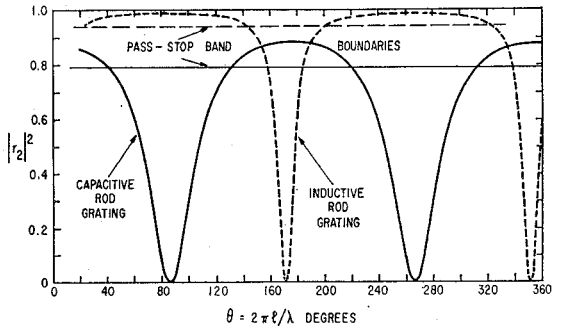

Fig. 13—Reflectivity versus (l) for capacitive and inductive rod gratings. No. of gratings (n)=2.

quite high throughout the range of θ corresponding to a stop band. In an accurate treatment the variation of the discontinuity reactances with wavelength must be considered, and (16) and (23) used to determine the reflectivity for different wavelengths. For comparison the effective propagation constant of a symmetrical element of the dielectric sheet-air space reflector system was calculated, taking the path lengths l in the dielectric and air equal. If ϵ is the dielectric constant, and $\theta_d = 2\pi l\epsilon^{1/2}/\lambda$, then for no dielectric loss,

$$\cosh \phi = (2\epsilon^{1/2})^{-1}[(\epsilon + 2\epsilon^{1/2} + 1)\cos^2\theta_d - (\epsilon - 1)]. \quad (29)$$

Fig. 11 shows such a curve for $\epsilon=4$, indicating that $\lambda/4$ is best as regards the air space and thickness of dielectric.

V. Conclusions

The transmission line treatment of the reflector problem, which is also applicable to the complete interferometer, indicates that the desired performance can be achieved in a number of ways. Reflectors consisting of quarter-wavelength dielectric sheets spaced quarter-wavelength apart are a good solution at longer wavelengths where the sheets are of reasonable thickness, although if a good dielectric such as fused quartz is used they are rather costly, and the size required leads to difficulties in fabrication. The new types of reflector structure considered such as stacked capacitive and inductive rod gratings are suitable structures for the interferometer. They are not too difficult to make, and can be made large without serious difficulty, this being especially so for the perforated metal plate gratings, which seems a good structure in all respects. Errors in the values of the equivalent reactances used for the discontinuities would only affect the reflectivity obtained from a given number of gratings and not the general method.

Resistive losses in the grating structures have been neglected, but although these will limit the ultimate reflectivity obtained by stacking gratings, it is expected that it will still be quite high. Optimum spacing of the gratings must be decided by deducing the effective propagation constant of the discontinuity involved, and the results on the gratings considered show that, depending on the type, either a half-wavelength or an odd quarter-wavelength spacing will be satisfactory. This also gives an indication of the bandwidth of the particular reflector system, the results indicting that this will be adequate. A more accurate treatment of this can be made, if necessary, using the appropriate equations and considering the variation of the reactances with wavelength.

Only dominant mode interaction between the discontinuities has been considered, and the dimensions of the structures must be such that higher-order modes are highly attenuated over the distance between gratings. While the amplitude of each mode will depend on the geometry of the discontinuity, it is felt that their effects will be small in the structures considered. The effect of any residual higher mode coupling would be to change the equivalent reactances,[16] not the general method of reflector design. Also the rod and strip grating structures considered depend on the polarization, but the perforated hole grating can be designed to work for any arbitrary polarized wave.

The ultimate reflectivity obtained will not be unduly sensitive to the dimensions of the rods, or hole diameter and plate thickness, provided a sufficient number of gratings is used. It is important, however, to maintain the required spacing and alignment of the rods or holes in the stacked gratings, and also to ensure that the gratings are parallel. As regards the complete interferometer, the sharpness of the fringes will be quite sensitive to the parallelism of the two reflectors.

Acknowledgment

The author would like to acknowledge the assistance derived from discussions with colleagues, Dr. D. M. Kerns and Dr. J. M. Richardson, on the various aspects of the work presented here.

[16] S. B. Cohn, "Analysis of the metal strip delay structure for microwave lenses," *J. Appl. Phys.*, vol. 20, pp. 257–262; March, 1949.